

## Electrochemical Deposition of Bright Nickel on Titanium Matrix from Ammoniacal Solution in the Presence of Thiourea

Liang Yuan<sup>1,2</sup>, Jiugang Hu<sup>1,\*</sup>, Zhiying Ding<sup>1</sup>, Shijun Liu<sup>1,\*</sup>

<sup>1</sup> School of chemistry and chemical engineering, Central South University, Changsha 410083, PR China.

<sup>2</sup> School of new energy science and engineering, Xinyu University, Xinyu 338004, PR China.

\*E-mail: [hjg.csu@gmail.com](mailto:hjg.csu@gmail.com), [shijunliu@csu.edu.cn](mailto:shijunliu@csu.edu.cn)

Received: 6 May 2017 / Accepted: 16 June 2017 / Published: 12 July 2017

The electrodeposition behaviors of nickel on titanium cathode were investigated in ammoniacal electrolyte in the absence and presence of thiourea. Tafel polarization curve and cyclic voltammogram studies demonstrate that with the presence of thiourea stimulates cathodic polarization and shifts the nucleation potential ( $E_{nu}$ ) towards more negative values. Moreover, the electrodeposition of nickel proceeds via 3D instantaneous nucleation whatever the presence of thiourea or not. There is noticeable improvement in surface morphology and deposit quality by introducing thiourea to the bath. Smooth and bright nickel deposits with small globular nickel crystals can be obtained when thiourea concentration is over 25 mg/L. The X-ray diffraction analysis indicates that thiourea can influence the crystallographic orientations of nickel crystals, thus improving the grain refinement and surface smoothness. Moreover, the effects of thiourea on the cathodic current efficiency (CE), energy consumption (EC) and kinetics parameters of cathodic process were also discussed. These results are beneficial for the nickel metallurgy or nickel plating in ammoniacal media.

**Keywords:** Nickel electrodeposition; Thiourea additive; Inhibiting nucleation; Bright surface

### 1. INTRODUCTION

Metal nickel or nickel coating can be electrodeposited from a variety of acidic electrolytes, including chloride system [1], sulfate system [2, 3] or a mixed system of chloride and sulfate [4, 5]. However, there is an unavoidable defect of severe hydrogen evolution on the cathode during electrodeposition from these acidic electrolytes, which will not only lower the current efficiency but also degrade the morphology of nickel surface with pitting or nodule. In recent years, nickel electrodeposition from ammonia-containing solution has been concerned due to the complex

characteristics between nickel ions and free  $\text{NH}_3$  [6]. Ammoniacal electrolytes are beneficial for obtaining high purity products, high current efficiency and fast deposition rate [7]. However, whatever the acidic baths or the ammoniacal electrolytes, there are some normal problems like poor surface finish, formation of pores and local pitting fault in the nickel deposits.

In general, in order to obtain metal deposits with good surface morphology, it is essential to introduce specific additives into the baths to modify the properties of electrolyte. Even a small amount of additive in the electrolyte can result in a noticeable quality change of final deposits. For nickel electrodeposition, various additives including glue, saccharin, sodium lauryl sulfate and so on can be used for improving brightness, reducing pitting corrosion, increasing hardness and suppressing the hydrogen evolution. For instance, Mohanty *et al* [8] found that sodium lauryl sulfate (SLS) acts as a good cathode polarizer to improve the surface morphology and deposit quality. Similar investigation was performed by Sekar [9] and Lu [2], who found that sodium lauryl sulfate as wetting agent can improve the hardness, surface morphology and corrosion resistance of the deposits. Ciszewski [10] obtained a good quality of nickel deposit and high current efficiency from a mixed of acidic chloride and sulfate bath by using saccharin together with ammonium salts as additive. Rudnik [4] reported on the electrochemical behavior of gluconate and found it is an efficient inhibitor for the growth of nickel moss and dendrites.

Thiourea (Tu) has been known as a cheap and environmentally safe additive and is most widely used in the electrolytic process of copper [11], zinc [12], nickel [13] and binary or ternary metal alloys [14, 15] from different baths. Benefited from its abundant functional groups, thiourea can be used to effectively control the metallic crystal shape and grain size, which can level the cathodic deposit surface. In industry, it is successfully used as a leveling and brightening agent for zinc [16] and copper [17] electrodeposition in acidic sulfate electrolyte. Meanwhile, Lin [18] found that nickel deposit obtained in the presence of thiourea exhibits relatively smooth, fine texture compared to coarse surface in the absence of thiourea. Cheong [19] observed that the addition of thiourea significantly improve the stability of the nickel bath and have a beneficial effect on the morphology of the nickel deposit. Zhu [20] and his co-workers found that the addition of thiourea into hydrophobic ionic liquids not only changes color of the electrolyte from yellow to yellow-green, but also changes the nucleation/growth process from instantaneous to progressive. Therefore, thiourea additive is desired to enhance the deposition process of nickel in ammoniacal electrolytes.

In view of the inherent merits of ammoniacal electrolyte and specific roles of thiourea additive, the present study focuses on the nickel electrodeposition process from ammoniacal electrolytes with or without thiourea. The electrochemical behaviors and nucleation process of nickel on titanium matrix have been in detail studied in the absence and presence of thiourea. The kinetic parameters such as Tafel slop ( $b$ ), transfer coefficient ( $\alpha$ ), exchange current density ( $i_0$ ) and diffusion coefficient ( $D$ ) are determined and discussed. Additionally, the deposit surface morphology, crystallographic orientations, the current efficiency and energy consumption have also been evaluated.

## 2. EXPERIMENTAL PART

All bath electrolytes were prepared by dissolving 0.5 mol/L nickel chloride ( $\text{NiCl}_2 \cdot 6\text{H}_2\text{O}$ ), 1.25 mol/L ammonium chloride ( $\text{NH}_4\text{Cl}$ ) and 2.0 mol/L ammonium hydroxide ( $\text{NH}_4\text{OH}$ ) in deionized water. The pH value was fixed at 8.10. In the bath electrolytes, the predominant nickel specie is  $\text{Ni}(\text{NH}_3)_4^{2+}$  according to the thermodynamic analysis [21]. In order to avoid deterioration of thiourea, the fresh solution of thiourea additive was prepared on a daily basis. All reagents are of analytical pure grade and used as received. Calculated amounts of thiourea were added to the electrolytic bath in aliquots from freshly prepared stock solution of 2 g/L.

All the electrochemical measurements were carried out in a conventional three electrode glass cell with 200 mL electrolyte using Galvanostat CHI660C (CH Instrument, China) electrochemical work station. All solutions used for electrochemical experiments were freshly prepared and high purity nitrogen was used to deaerate the dissolved oxygen to keep an inert atmosphere prior to each electrochemical measurement. The working electrode was a square titanium electrode (10 mm  $\times$  10 mm) enclosed in epoxy resin. Platinum plate was used as auxiliary electrode, the area of which is twice as large as the working electrode. The saturated calomel electrode (SCE), mounted inside a Luggin capillary, was used as the reference electrode. The working electrode was closed to the Luggin capillary as much as possible and therefore the Ohmic drop could be neglected. Prior to each electrochemical measurement, the electrode surface were mechanically polished with successively finer grades of emery paper, and then polished with 0.05  $\mu\text{m}$   $\text{Al}_2\text{O}_3$  powder. The polished working electrode was washed with acetone and alcohol, and then dried in air. Both cyclic voltammetry and Tafel curves were scanned at a rate of 10 mV/s. From the cathodic polarization curves for nickel deposition, Tafel slopes were determined and transfer coefficients were calculated by using the following Eqs. (1)-(3).

$$\eta = a + b \log i \quad (1)$$

$$b = \frac{2.3RT}{\alpha nF} \quad (2)$$

$$a = -\frac{2.3RT}{\alpha nF} \log i_0 \quad (3)$$

where  $\eta$  is the overpotential (V),  $a$  is the intercept,  $b$  is the Tafel slope (V/decade),  $R$  is the ideal gas constant (8.314 J/mol·K),  $T$  is the temperature (K),  $F$  is the Faraday's constant (96485 C/mol),  $\alpha$  is the transfer coefficient,  $i_0$  is the exchange current density and  $I$  is the current density ( $\text{mA}/\text{cm}^2$ ).

Nickel electrodeposition was carried out in a rectangular flow cell made from perspex, which could hold approximately 2 L nickel electrolyte. The flow rate of the electrolyte was kept at 2 L/h and the working temperature was 50 °C. Pure titanium substrate with an area of 10  $\text{cm}^2$  was used as cathode and high pure graphite plate was used as anode. The surface of titanium electrode prior to nickel deposition was polished with 400 and 1200 grade silicon carbide paper. Then the polished cathode was rinsed in 1 mol/L HCl solution and followed by washing with deionized water. All the electrodeposition experiments were conducted for 1 h at a constant current density of 400  $\text{A}/\text{m}^2$  by applying current from a regulated power supplier (0-30 V , 10 A, dc. power supply). A precise voltage meter was used to record the cell voltage (CV). At the end of the electrolysis period, the weight of cathode was accurately obtained after washed and dried in air. The cathodic currency efficiency for

nickel electrodeposition was calculated gravimetrically according to Eq. (4) by comparing the actual deposit weight to the theoretical mass on the cathode.

$$\eta_{Ni} = \frac{m - m_0}{qIt} \times 100\% \quad (4)$$

Where  $\eta_{Ni}$  (%) is the current efficiency of nickel,  $q$  is the electrochemical equivalent of nickel,  $I$  is the current (A),  $t$  is the electrodeposition time (h),  $m$  is the total mass of cathode (g) when electrolyzed for  $t$  hour and  $m_0$  is the mass of pure cathode (g).

The energy consumption for electrolyzing nickel can be calculated by Eq. (5):

$$E = \frac{UIt}{m - m_0} \quad (5)$$

where  $E$  (kWh/kg) is the energy consumption,  $U$  (V) is the average cell voltage.

X-ray diffraction analysis was carried out using X-ray diffractometer (model Rigaku D/max 2550) with Cu-K $\alpha$  radiation ( $\lambda=0.15406$  nm) working at 30 mA and 40 kV to study the preferred crystal orientations of nickel deposits. The diffractograms were obtained in the  $2\theta$  rang of  $10^\circ$ - $100^\circ$  using a  $0.02^\circ$  step and acquisition time of 2 s/step. The microscopic morphology and elemental analysis of nickel samples were performed by scanning electron microscopy (model XL30-ESEM) equipped with energy dispersive spectroscopy (EDS).

### 3. RESULTS AND DISCUSSION

#### 3.1 Cyclic voltammetric (CV) studies

The electrochemical behaviors of nickel on titanium substrate in the absence and presence of thiourea were analyzed using cyclic voltammetry. Fig. 1 depicts the voltammogram curves at different concentrations of thiourea. It can be seen that the cathodic peak potential is shifted to more negative value and the peak current decreases as increasing thiourea concentration. The potential where nickel electrodeposition occurred on the titanium substrate is defined as the nucleation potential ( $E_{nu}$ ) in the cyclic voltammetry curves. On switching the scanning direction to positive, a typical crossover loop is observed, suggesting a nucleation process [22]. This phenomenon are also observed in zinc [23] electrodeposition from ammoniacal electrolyte and can be inferred that nickel electrodeposition on titanium electrode requires an overpotential to initiate nucleation and maintain growth of nickel because of the inherent high polarization property of the ammonia solution. The point of zero current is referred to as the crossover potential denoted by  $E_{co}$ . The potential difference between the nucleation potential ( $E_{nu}$ ) and cross overpotential ( $E_{co}$ ) is determined as the nucleation overpotential (NOP), which can be regarded as an indicator of the extent of polarization of a cathode [16]. As seen in Table 1, the deposition overpotential is sensitive to thiourea additive, where the NOP value increases with the content of thiourea in the baths. For example, the NOP value increased by 61 mV with 100 mg/L thiourea compared with the blank electrolyte. The large NOP value indicates a stronger interaction of thiourea occurred on the cathode surface. At the high thiourea concentrations, due to the strong adsorption, the active sites for nickel deposition on cathode surface are blocked and a higher driving

force for the nickel complex ion reduction would be required. This results agree well with the previous studies about thiourea on nickel electrodeposition in acidic system [20,24], which also found that thiourea exhibited different behaviors at various concentrations.

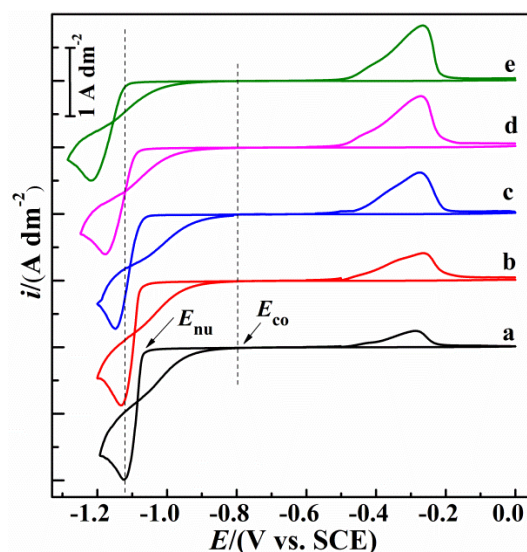


**Figure 1.** Cyclic voltammograms of nickel deposition from ammoniacal solutions in the absence and presence of thiourea: (a) blank; (b) 10 mg/L; (c) 25 mg/L; (d) 50 mg/L; (e) 100 mg/L. Scan rate is 50 mV/s.

**Table 1.** Effect of thiourea on the cross overpotential ( $E_{co}$ ), nucleation potential ( $E_{nu}$ ) and nucleation overpotential (NOP) of nickel deposition from ammoniacal solutions

Thiourea (mg/L)	$-E_{co}$ (mV)	$-E_{nu}$ (mV)	NOP (mV)
Blank	891	1050	159
10	882	1052	170
25	886	1061	175
50	889	1077	188
100	890	1110	220

### 3.2 Nucleation study

The chronoamperometry was used to investigate nickel nucleation mechanism at different concentration of thiourea in the potential range from -1.11 to -1.05 V vs SCE. The potentials were selected from the corresponding CV curves to sufficiently initiate the nucleation and growth of nickel crystals [25]. The current-time transient curves are shown in Fig. 2. The cathodic current increases sharply up to a maximum value ( $i_m$ ) in a very short time, which corresponds to the nucleation process. Afterward, the current decays gradually due to the relaxation of diffusion layer. All the transients show the same characteristic, which is typical diffusion-limited nucleation with three-dimensional growth process. The main difference is the maximum current peak ( $i_{max}$ ) and the time to reach the maximum

current peak ( $t_{\max}$ ). The  $i_{\max}$  is higher and the  $t_{\max}$  is shorter while the applied potential shifts to more negative values. Meanwhile, the  $i_{\max}$  is lower at the same potential in the presence of thiourea, which indicates that the thiourea can hinder the nucleation of nickel.

The nucleation mechanism of nickel was further elucidated by analyzing the chronoamperometric curves with the models proposed by Scharifker and Hills [26], that is instantaneous (Eq. (6)) and progressive (Eq. (7)) three-dimensional nucleation models.

$$\left(\frac{I}{I_m}\right)^2 = \frac{1.9542}{t/t_m} \left\{ 1 - \exp \left[ -1.2564 \left( \frac{t}{t_m} \right) \right] \right\}^2 \quad (6)$$

$$\left(\frac{I}{I_m}\right)^2 = \frac{1.2254}{t/t_m} \left\{ 1 - \exp \left[ -2.3367 \left( \frac{t}{t_m} \right)^2 \right] \right\}^2 \quad (7)$$

Where  $i_m$  and  $t_m$  are the values of  $i$  and  $t$  at the maxima in the transients, respectively. The instantaneous nucleation corresponds to a slow growth rate of nuclei on a certain active sites and nuclei activation at the same time. Whereas, the progressive nucleation has a fast growth rate of nuclei on any active sites and activated during the course of electrodeposition [27].

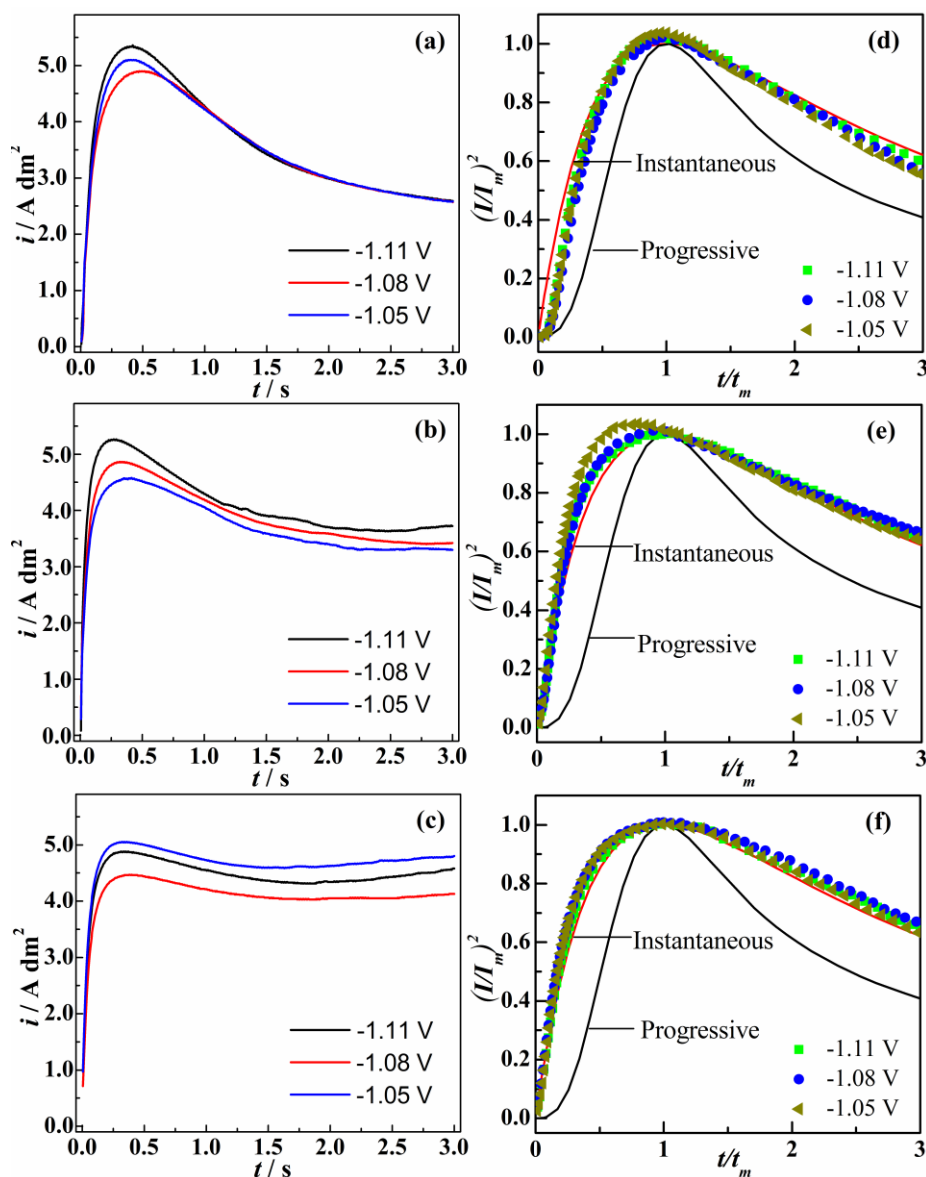
As shown in Fig. 2, the experimental transients were normalized and then compared to the theoretical curves derived from two limiting nucleation mechanisms. It is obviously that the experimental results in both absence and presence of thiourea agree well with the instantaneous model. Therefore, the electrocrystallization process of nickel is governed by 3D instantaneous nucleation process and is not affected by the existence of thiourea. However, Zhu [20] reported that the nucleation/growth process of Ni is changed from 3D instantaneous nucleation to 3D progressive nucleation on copper substrate after addition of thiourea into hydrophobic ionic liquid electrolyte. The diffusion coefficient of active species can be determined by the slop of chronoamperograms in  $i$  versus  $t^{-1/2}$  coordinates according to Cottrell equation (Eq.(8)) [28].

$$i = \frac{nFAD^{1/2}C_0}{\pi^{1/2}t^{1/2}} \quad (8)$$

Where  $i$  is the current,  $n$  the number of electrons involved,  $F$  the Faraday constant,  $A$  the active area of the electrode,  $D$  the diffusion coefficient,  $C_0$  the concentration of species in the bulk, and  $t$  the time. The Cottrell equation describes the changes of current along with time in the unsteady-state diffusion-limited condition. Each of the transients exhibits the common characteristic that current promptly decays to the steady-state after peak current. From Table 2, as a whole, it is clear that the electrolyte without thiourea has a slightly higher diffusion coefficient rate compared those with thiourea at the same potential. Cao *et al* [6] reported an approximate diffusion coefficient value of  $1.0 \times 10^{-6}$  from ammoniacal Ni(II) electrolyte on glassy carbon electrode surface without thiourea, which was slightly higher than that of in the presence of thiourea. Thus, the nickel complexes in the present of thiourea are expected to move slower than those without thiourea, which indicates that thiourea could hinder the nucleation process of nickel and result in the formation of nickel crystals more difficult.

**Table 2.** Diffusion coefficients of Ni(II) at different concentrations of thiourea

Blank		20 mg/L		50 mg/L	
Potential (V)	$D$ (cm <sup>2</sup> /s)	Potential (V)	$D$ (cm <sup>2</sup> /s)	Potential (V)	$D$ (cm <sup>2</sup> /s)
-1.11	$1.78 \times 10^{-6}$	-1.11	$9.15 \times 10^{-7}$	-1.11	$8.57 \times 10^{-7}$
-1.08	$2.69 \times 10^{-6}$	-1.08	$1.45 \times 10^{-6}$	-1.08	$9.38 \times 10^{-7}$
-1.05	$2.89 \times 10^{-6}$	-1.05	$1.63 \times 10^{-6}$	-1.05	$8.82 \times 10^{-7}$

**Figure 2.** Experimental current-time transient curves and the corresponding non-dimensional plots of  $i/I_{\max}$  versus  $t/t_{\max}$  according to the Scharifker-Hills' nucleation models for nickel electrodeposition in the absence and presence of thiourea at different potentials. (a,d) blank; (b,e) 25 mg/L thiourea; (c,f) 50 mg/L thiourea.

### 3.3 Polarization study

Fig. 3 depicts cathodic polarization curves for nickel electrodeposition over the thiourea concentration range of 0 to 100 mg/L. It can be seen that the presence of thiourea in the electrolytes can activate cathode surface by shifting the deposition potentials towards more negative values. As increasing thiourea concentration, the polarization effect is more obvious. This phenomenon can be attributed to the adsorption of thiourea on the cathode surface, which alters the double layer structure and decreases the rate of electrochemical reaction. Opposite result was obtained in Mohanty's [24] research, which displayed that depolarization of the cathode occurs at low concentration of thiourea (<20 mg/L) due to both the adsorption of thiourea and interaction of thiourea molecule with  $\text{Ni}^{2+}$  in sulfuric acid system. The electron transfer kinetic parameters for nickel deposition on titanium substrate including Tafel slop ( $b$ ), transfer coefficients ( $\alpha$ ) and the exchange current density ( $i_0$ ) were calculated from the cathodic polarization curves by Eqs. (1)-(3). The results are listed in Table 3. In the absence of thiourea, the value of  $\alpha$  and  $b$  is 0.228 and -131 mV/decade, respectively. However, as the amount of added thiourea increases, the transfer coefficient decreases and the Tafel slop increases accordingly. At 100 mg/L thiourea, the values of  $\alpha$  and  $b$  are 0.178 and 165 mV/decade, respectively. This result is in agreement with the study of Stankovic *et al* [29] which also found that the transfer coefficient decreases with increasing thiourea content during copper electrodeposition in sulfate solution. In addition, all the Tafel slop values are larger than -120 mV/decade, suggesting that the charge transfer mechanism of the deposition process is quite complex, not just a simple electron transfer [11]. Meanwhile, the exchange current density could more clearly reflect the effect of thiourea on nickel deposition process. It can be seen from Table 3 that the  $i_0$  value decreases with the increase of thiourea concentration from 0 mg/L to 100 mg/L. The decrease of  $i_0$  reflects that thiourea can slow down the rate of electron transfer reaction due to the adsorption of thiourea on the cathode surface, thus making nickel electrodeposition reaction more difficult.

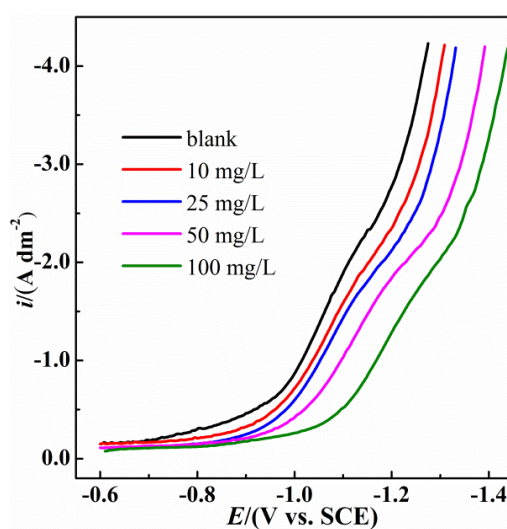


**Figure 3.** Cathodic polarization curves of nickel deposition in the presence of thiourea.



**Table 3.** Effect of thiourea on the kinetics parameters for nickel deposition.

Thiourea (mg/L)	Tafel slop, $b$ (mV/decade)	Transfer coefficient, $\alpha$	$i_0 \times 10^{-3}$ (mA/cm <sup>2</sup> )
Blank	-131	0.228	3.020
10	-136	0.216	2.512
25	-145	0.203	1.778
50	-151	0.196	1.047
100	-165	0.178	0.935

### 3.4 Surface quality and crystallographic orientations

A series of optical images and SEM photomicrographs of nickel deposits were obtained at the constant current density of 400 A/m<sup>2</sup> for 1 h from ammoniacal electrolytes. As shown in Fig. 4, thiourea has dramatic effect on the interfacial deposition behaviors of nickel. All the shape of grain has a round or globular feature as a whole, which is quite different from the blade shape obtained on stainless steel substrate by Cao[6]. In the electrolyte without thiourea, the nickel deposit is loose and composed of spherical particles with the diameter below 0.5  $\mu\text{m}$  (Fig. 4b). Addition of thiourea does not have any effect on the shape of the crystals, but refines the grain size obviously. Meanwhile, thiourea improves the formation of bright and smooth deposits. When the concentration of thiourea is larger than 25 mg/L, the uniform, dense and compact nickel deposits with the smallest crystal can be obtained. Moreover, it is clear that the nickel surface is slightly gray in the presence of high content thiourea as shown in Figs. 4g and 4i. This might be attributed to the incorporation of sulfur at the deposit surface and the result was confirmed by EDS analysis as shown in the inset of Fig. 4j. Mohanty [24] also reported that an increase in the thiourea concentration in the acidic sulfate bath progressively increases sulfur content in the nickel deposit because of either the decomposition products of thiourea or the inclusion of sulfur in the form of precipitated black NiS. Meanwhile, very low incorporation of sulfur also existed in copper [30] coating in the form of CuS and in zinc [31] final deposits in Zn(NO<sub>3</sub>)<sub>2</sub> electrolyte while using thiourea as additive. Several mechanisms were proposed to explain the formation of the sulfur compounds [24], including the oxidation of thiourea to form H<sub>2</sub>S and sulfur (S), the reduction of thiourea to H<sub>2</sub>S and NH<sub>4</sub>CN, the decomposition of thiourea to elemental S and the hydrolysis of thiourea to form CO(NH<sub>2</sub>)<sub>2</sub> and H<sub>2</sub>S. However, these proposed mechanisms were unconfirmed absolutely, but one thing for sure was that sulfur atom reached into the nickel deposit in some way. The sulfur in nickel deposit from ammoniacal electrolytes is more inclined to originate from the decomposition of partial thiourea molecules because the C=S bond of thiourea could more easily break to form S<sup>2-</sup> in basic media and then interact with nickel on the surface of deposits.

Fig. 5 and Table 4 illustrate the XRD results of nickel deposits from ammoniacal solutions in the absence and presence of thiourea additive. It was obvious that the deposits have four crystal planes including (111), (200), (220) and (311). The (111) plane is the most preferred crystal orientation. The addition of thiourea does not change the preferred crystal plane but results in change of relative peak intensities of other crystal planes. Increasing the concentration of thiourea leads to a significant rise in the peak intensity of (200) plane. The crystal growth in the direction of both (220) and

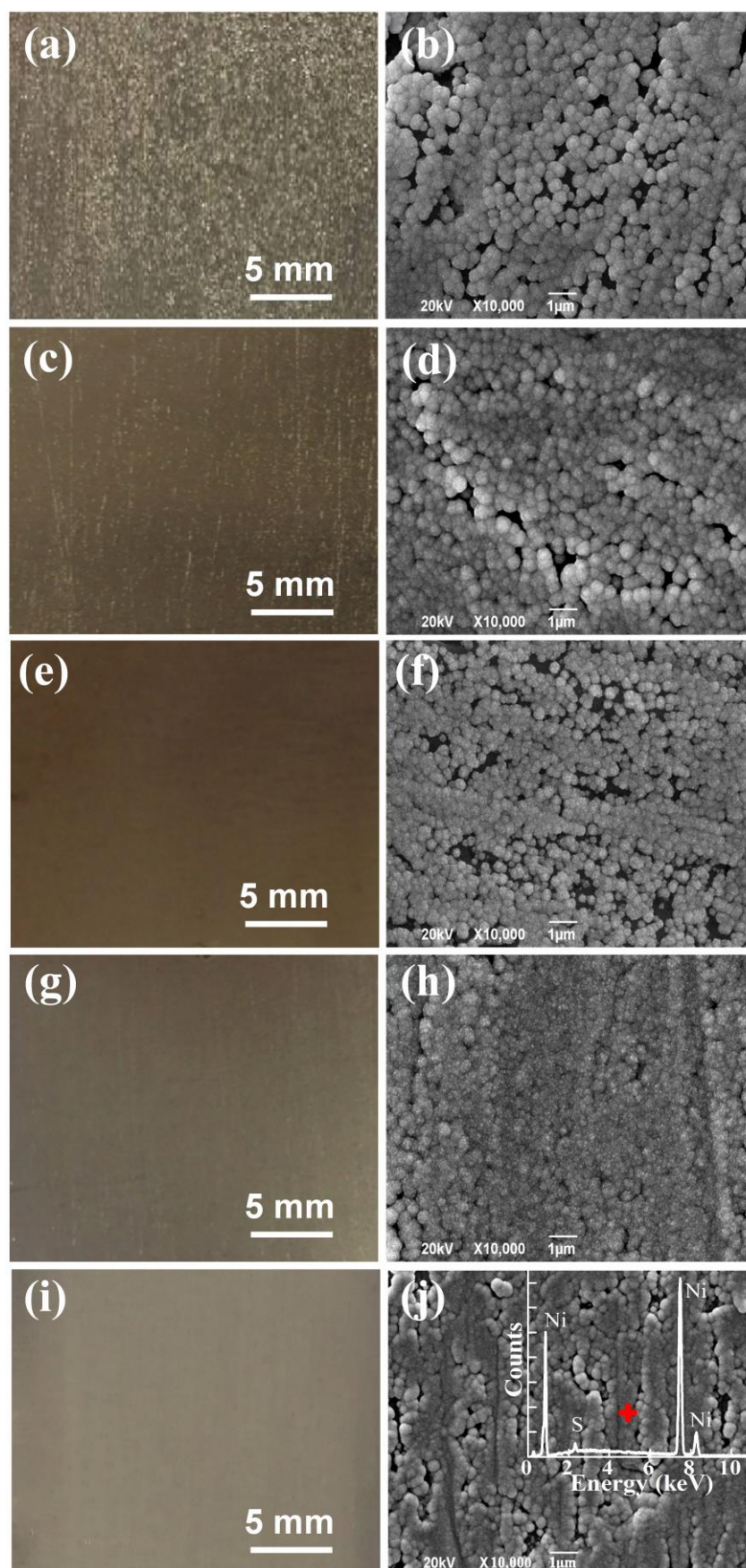


**Figure 4.** Optical images and SEM photomicrographs of nickel deposits in the presence of thiourea. (a, b) blank; (c, d) 10 mg/L; (e, f) 25 mg/L; (g, h) 50 mg/L; (i, j) 100 mg/L.

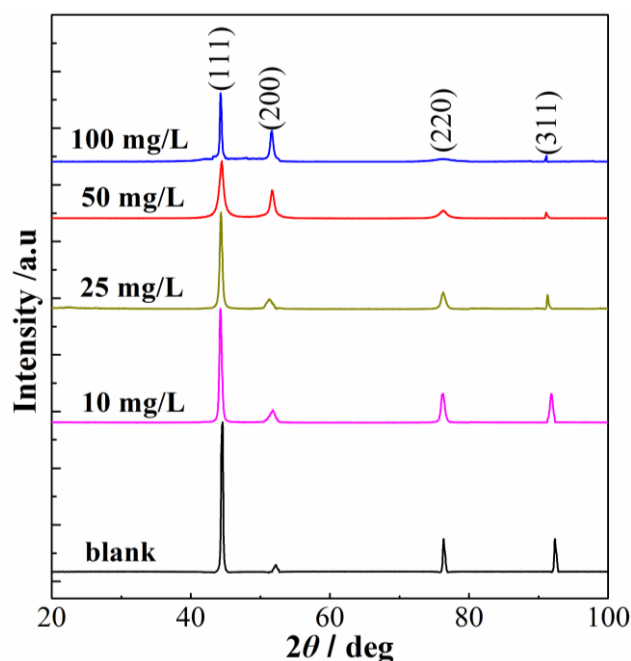


**Figure 5.** X-ray diffraction patterns of nickel deposits obtained in the presence of thiourea.

(311) planes is inhibited obviously. These marked changes in the crystallographic orientations result in the formation of smooth and compact nickel deposits with small particles [27]. Thiourea is a well-known grain refining agent and composed of one sulfur atom and two  $-NH_2$  groups. The thiourea molecules can be selectively adsorbed on the active sites of crystals and inhibit the random orientation of nickel crystals at low concentration [6,24]. With the increase of thiourea concentration, the electrode surface is partially covered by the absorbed thiourea, which blocks the active electrode sites and slows down the growth rate of crystals, resulting in the fine-grained nickel deposits. At high concentration of thiourea, the high electrode coverage and strong interaction could be occurred. Moreover, the absorbed thiourea might coordinate with nickel at high concentration. Therefore, the inhibition role of thiourea on nickel deposition could be attributed to thiourea adsorption or the formation of  $Ni(Tu)_n^+$  complexes.

**Table 4.** Effect of thiourea on crystallographic orientations of nickel deposits

Thiourea (mg/L)	Relative peak intensity of nickel crystal orientations ( $I/I_{max}$ )/%			
	(111)	(200)	(220)	(311)
Blank	100	15.8	25	16
10	100	18.2	16.7	12.5
25	100	22.2	11	10
50	100	24.8	8.9	8.1
100	100	25.8	5.4	8.6

### 3.5 Current efficiency and energy consumption

The effect of thiourea on the current efficiency (CE) and energy consumption (EC) for nickel electrodeposition is shown in Fig. 6. The CE is 90.15% in the absence of thiourea and slightly increases *ca.* 3% with the increase of thiourea concentration up to 10 mg/L. This could be closely related to the role of thiourea by adsorbing on the cathode surface and blocking hydrogen activation sites. Under this low concentration of thiourea, the adsorption was so weak that no adsorption layer is formed. Herein the main role of thiourea is to increase the overpotential of hydrogen evolution, suppress hydrogen evolution and reduce the side reactions. Some authors thought the strong adsorption of thiourea molecules on electrode surface is to reduce gas evolution [19]. However, another point is that thiourea just only act as the transfer medium at a certain concentration and accelerate the deposition rate [20]. Further increasing the thiourea concentration decreases CE significantly. When the concentration of thiourea reaches 100 mg/L, the CE decreases rapidly to a low value of below 80%. This result is slightly different from Mohanty's observation, which depicted that the current efficiency decrease when increasing thiourea concentration over a range of 0 to 40 mg/L [24]. The corresponding trends of EC is just the opposite of CE. The decrease in CE might be attributed to the strong adsorption of thiourea molecules on cathode surface to form an adsorption layer, which inhibits the mass transfer process and restricts the electroreduction of nickel ammonia complex ions at the cathode. Mouanga [32] have compared the adsorption behaviors of thiourea on metal surface with urea and guanidine and found that the adsorption of thiourea could interact with metal substrate through the C=S bond due to the electronic polarization of thiocarbonyl group. The strong adsorption of thiourea on cathode surface requires a higher driving force for electroreduction, hence the energy consumption increases as the increase of the cell voltage.

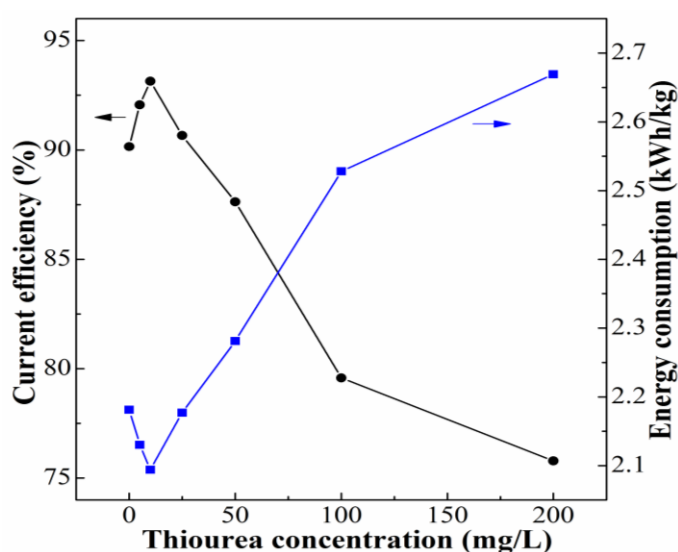


**Figure 6.** Effect of thiourea on current efficiency (CE) and energy consumption (EC) during nickel deposition.

#### 4. CONCLUSIONS

Effects of thiourea over a concentration range of 0 to 200 mg/L on nickel electrodeposition from ammoniacal solutions were investigated. The chronoamperometry shows that the nickel nucleation processes via 3D instantaneous nucleation whether or not with thiourea, but slightly lowers the diffusion coefficient rates and hinders the nucleation process. Cyclic voltammetry and Tafel plot study reveal that thiourea stimulates the cathodic polarization and increases the Tafel slop. A progressive decrease in the rate of transfer coefficients and the exchange current density on titanium substrate were also observed when increasing thiourea concentration. SEM results show that the increase of thiourea concentration has any effect on the shape of nickel crystals, but changes the grain size and deposit quality obviously. When the thiourea content is larger than 25 mg/L, the uniform, dense and bright nickel deposit with the small crystals can be obtained. XRD results indicate that the presence of thiourea does not change the most preferred (111) crystal plane, but inhibits the crystallite growth of (220) and (311) planes. The results indicate that higher concentration of thiourea (>25 mg/L) in the electrolyte dramatically reduces the cathodic current efficiency and hence increases the energy consumption.

#### ACKNOWLEDGMENTS

This work was financially supported by the National Basic Research Program of China (2014CB643401) and the National Natural Science Foundation of China (51134007, 51404299).

#### References

1. M. Boubatra, A. Azizi, G. Schmerber and A. Dinia, *Ionics*, 18 (2012) 425.
2. L.U. Jing, Q.H. Yang and Z. Zhang, *T. Nonfer. Metal Soc.*, (2010) 97.
3. Y. Jin, H. Yu, D. Yang and D. Sun, *Rare Metals*, 29 (2010) 401.
4. E. Rudnik, M. Wojnicki and G. Włoch, *Surf. Coat. Tech.*, 207 (2012) 375.
5. F. Lantelme, A. Seghioeur and A. Derja, *J. Appl. Electrochem.*, 28 (1998) 907.
6. H. Cao, D. Yang, S. Zhu, L. Dong and G. Zheng, *J. Solid State Electrochem.*, 16 (2012) 3115.
7. H.Z.C. Guo Qu Zhen, *T. Nonfer. Metal Soc.*, 13 (2003) 217.
8. U.S. Mohanty, B.C. Tripathy, S.C. Das, P. Singh and V.N. Misra, *Hydrometallurgy*, 100 (2009) 60.
9. R. Sekar, K.K. Jagadesh and G.N.K.R. Bapu, *Korean J. Chem. Eng.*, 32 (2015) 1194.
10. A. Ciszewski, S. Posluszny, G. Milczarek and M. Baraniak, *Surf. Coat. Tech.*, 183 (2004) 127.
11. F.C.W.S. E. E. Farndon, *J. Appl. Electrochem.*, 25 (1995) 574.
12. M.C. Li, L.L. Jiang, W.Q. Zhang, Y.H. Qian, S.Z. Luo and J.N. Shen, *J. Solid State Electrochem.*, 11 (2007) 549.
13. R.F. Renner and K.C. Liddell, *J. Appl. Electrochem.*, 32 (2002) 621.
14. M. Mouanga, L. Ricq and P. Berçot, *J. Appl. Electrochem.*, 38 (2008) 231.
15. E. Feng, Z. Wang, X. Zhu, Q. Liu and J. Wang, *J. Electrochem. Soc.*, 159 (2012) 842.
16. D.J. Mackinnon, J.M. Brannen and R.M. Morrison, *J. Appl. Electrochem.*, 18 (1988) 252.
17. L. Muresan, S. Varvara, G. Maurin and S. Dorneanu, *Hydrometallurgy*, 54 (2000) 161.
18. K.-L. Lin and J.-W. Hwang, *Mater. Chem. Phys.*, 76 (2002) 204.
19. W.J. Cheong, B.L. Luan and D.W. Shoesmith, *Appl. Surf. Sci.*, 229 (2004) 282.
20. Y.L. Zhu, Y. Katayama and T. Miura, *Electrochim. Acta*, 85 (2012) 622.
21. I. Rodriguez-Torres, G. Valentin and F. Lapicque, *J. Appl. Electrochem.*, 29 (1999) 1035.

22. U.S. Mohanty, B.C. Tripathy, P. Singh and, S.C. Das, *J. Appl. Electrochem.*, 38 (2008) 239.
23. Z.M. Xia, S.H. Yang and M.T. T, *RSC Adv.* 5(2015) 2663.
24. U.S. Mohanty, B.C. Tripathy, S.C. Das and V. N. Misra, *Metall. Mater. Trans. B*, 6 (2005) 737.
25. M. Bernarda, I.V. Cecilia and I. Gabriela, *J. Electroanal. Chem.*, 6 39(2010)95.
26. H.G. Scharifker B, *Electrochim. Acta*, 28 (1983) 879.
27. L.K.Wu, W.K.Wang, H.Z.Cao, G.Y.Hou, Y.P.Tang and G.Q.Zheng, *J. Electrochem. Soc.* 163 (2016) D829
28. D. Grujicic, B. Pesic, *Electrochim. Acta*, 50 (2005) 4426.
29. Z.D. Stankovic, M. Vukovic, *Electrochim. Acta*, 41 (1996) 2529.
30. B. Tadesse, M. Horne and J. Addai-Mensah, *J. Appl. Electrochem.*, 43 (2013) 1185.
31. S. Gallanti, E. Chassaing, D. Lincot and N. Naghavi, *Electrochim. Acta*, 178 (2015) 225.
32. M. Mouanga, L. Ricq and P. Bercot, *J. Appl. Electrochem.*, 37 (2007) 283.

© 2017 The Authors. Published by ESG ([www.electrochemsci.org](http://www.electrochemsci.org)). This article is an open access article distributed under the terms and conditions of the Creative Commons Attribution license (<http://creativecommons.org/licenses/by/4.0/>).